environments

MDPI

Article

Porous Geopolymer Insulating Core from a Metakaolin/Biomass Ash Composite

Annalisa Natali Murri [1,*], Valentina Medri [1], Elettra Papa [1], Luca Laghi [2], Claudio Mingazzini [3] and Elena Landi [1]

1 CNR-ISTEC, National Research Council-Institute for Science and Technology for Ceramics, via Granarolo, 64-48018 Faenza, Italy; valentina.medri@istec.cnr.it (V.M.); elettra.papa@istec.cnr.it (E.P.); elena.landi@istec.cnr.it (E.L.)
2 CertiMaC ScarL, via Granarolo, 62-48018 Faenza, Italy; l.laghi@certimac.it
3 ENEA SSPT/PROMAS TEMAF, Laboratory of Materials Technologies Faenza, Department for Sustainability/Division Sustainable Materials, Italian National Agency for New Technologies, Energy and Sustainable Economic Development, via Ravegnana, 186-48018 Faenza, Italy; claudio.mingazzini@enea.it
* Correspondence: annalisa.natalimurri@istec.cnr.it; Tel.: +39-0546-699-776

Received: 20 October 2017; Accepted: 28 November 2017; Published: 1 December 2017

Abstract: Ashes derived from the combustion of vegetal and animal biomass still represent a mostly unexplored secondary raw material for the production of alkali-activated materials, given their peculiar chemical nature. In this work, calcium phosphate biomass ashes were successfully used as partially reactive fillers in a metakaolin-based geopolymer composite to produce, by direct foaming, sustainable and lightweight boards with thermal insulating properties. The investigated materials were obtained by activating a blend of metakaolin and biomass ash in a weight ratio of 1: 1 and foamed with the addition of H_2O_2 in measure of 5 wt. %, to maximize the volume of disposed ash and ensure adequate properties to the material at the same time. The obtained geopolymer composite was characterized by microstructural, chemical-physical, mechanical and thermal analysis: the obtained results showed that biomass ash and metakaolin well integrated in the microstructure of the final porous material, which was characterized by a density of about 310 kg/m^3 and a thermal conductivity of 0.073 W/mK at a mean test temperature of 30 °C, coupled with an acceptable compressive strength of about 0.6 MPa. Dilatometric and thermogravimetric analysis, performed up to 1000 °C, highlighted the thermal stability of the composite, which could be regarded as a promising material for low-cost, self-bearing thermal insulating partitions or lightweight cores for thermostructural sandwich panels.

Keywords: geopolymer; biomass ash; composite; thermal insulation; sandwich panel; waste materials

1. Introduction

In recent years, the need to limit the consumption of natural, non-renewable resources and to progressively lower the energy demand has led to the design of sustainable and environmentally-friendly materials, technologies and processes. Two of the major industrial branches in terms of impact on global emissions and energy consumption, namely the construction and transportation sectors, are increasingly asked to prioritize ecological manufacturing processes and firmly integrate recyclability in the design phase of any component, to produce value-added sustainable solutions.

Thermal insulating elements are above all able to improve the energetic performance of both buildings and means of transport, therefore finding an ideal balance between different needs and requirements is a crucial point for future developments [1–3]. In the frame of designing low-weight insulating materials and flame-resistant barriers for buildings and vehicles, the development of

multi-functional materials, able to couple energy efficiency with fire safety represents one of the main aims of the research [3–5].

Insulating and flame-resistant materials have been recently developed as greener alternatives to the more traditional petrochemical-derived solutions [6]: an increasing use of renewable resources and new manufacturing processes integrating wastes are being largely adopted in the production of insulating products [1,4,7–9]. Nevertheless, fully meeting the technical and safety requirements and at the same time reducing the environmental impact of the manufacturing process still represents an issue to address.

Flame resistant inorganic materials based on alkali-activated aluminosilicates, namely geopolymers, have been proposed as a valid alternative for organic polymer matrix replacement in fibre-reinforced composite panels for aircrafts interiors, reducing the fire hazards using a low-cost and sustainable material [10]. Geopolymers are produced by reacting an aluminosilicate powder with a highly concentrated alkali solution [11–13] and, may act as a binder for different fillers, producing various composite materials. Geopolymer composites can meet many of the ideal characteristics of lightweight materials for the building and transportation sectors, such as non-flammability, high temperature resistance, chemical resistance against acids and alkalis, durability, safety for human health and low carbon footprint [4,12,14]. For such remarkable properties, geopolymers and geopolymer composites have been widely investigated for the design of insulating materials in buildings and constructions, exploiting their intrinsic porosity eventually coupled with an induced macro-porosity by direct foaming [15–21].

As well as being excellent candidates for the development of thermal insulating and flame-resistant products, geopolymers have the advantage that they can be obtained from a wide range of by-products and waste materials, including coal combustion ashes, biomass ashes, metallurgical slags, construction and demolition wastes and the like, having therefore a negligible impact on the environment [7,9,22]. Among them, ashes derived from the combustion of vegetal and animal residues still represent an understudied source material for the production of alkali activated materials, given their peculiar chemical nature largely based on calcium phosphates, alkali sulphates and chlorides and only secondarily on reactive aluminosilicates [23,24]. Indeed, animal-derived biomass ashes are generally landfilled or used in very limited amounts as fertilizers or as partial addition to Portland cements and an environmental friendly and economically viable solution for their massive disposal or recycling is still needed.

In this work waste biomass ashes were regarded as a source material for the production of a novel low-cost material able to represent a promising alternative for the development of a sustainable thermal insulating system. The completely inorganic nature of the designed material ensures significant high temperature stability, while the application of a direct foaming technique allows to easily build up a tailored pore network to foster its insulation ability without excessively affecting its mechanical properties. The designed material is therefore capable of meeting both environmental and performance needs and might be successfully used as a self-bearing partition or as a lightweight core for thermostructural sandwich panels, in conjunction with flame resistant skins made of fibre reinforced ceramic laminates [25]. The overall properties of the material and its easy and sustainable production process potentially make it a promising solution for applications in the construction and transportation industries.

2. Materials and Methods

2.1. Raw Materials

An ultrafine metakaolin powder (Argical M-1200S from Imerys, France, D50 = 2 μm, SiO_2 = 55%, Al_2O_3 = 39%, specific surface area = 19 m^2/g, coded MK) was used to formulate the geopolymer composite, which was reacted with an aqueous potassium poly-silicate solution (KSil 35-35, Ingessil

Industria Silicati, Italy), appositely modified (coded KS23) to obtain a molar ratio H_2O: K_2O = 23 and SiO_2: K_2O = 2 by dissolving KOH pellets with purity > 85% (Sigma-Aldrich, Saint Louis, MO, USA).

A blend of five different biomass ashes from a power plant located in Faenza (Tampieri Energie S.r.l., Faenza, Italy) was used as a partially reactive filler in the composite formulation. All the ashes came from the combustion of residues of both vegetal and animal derived wastes and were previously mixed together in weight ratios corresponding to the yearly production of each ash type by the plant, with the aim to maximize the total volume of disposed material. After mixing, the obtained ash blend was ground and sieved to obtain a particle size < 250 µm. Then, as part of the blend consisted of humidified extinguished ashes, it was thermally re-treated for 1 h at 900 °C, a temperature similar to that used in the plant process [23] to eliminate any organic residual or unburnt material, which may negatively affect the geopolymerization process (coded BM). This step, carried out to remedy the uneven processing of the ashes coming directly from the plant, was specifically required for the lab-scale experimental activities but could be more easily replaced at the industrial scale by controlling the upstream plant process and the temperatures involved, making all the ash types directly recyclable.

The treated biomass ash blend is mainly characterized by large amounts of calcium-phosphate phases (mainly hydroxyapatite), lower amounts of calcium silicates and calcium hydroxide and fewer traces of alkali chlorides and sulphates phases (Figure 1). Accordingly, the elemental composition of the powder blend highlights Ca, P, K and Si as the main elements, being Al detected only in negligible amounts (Table 1).

Hydrogen peroxide solution 30 wt. % in H_2O by Sigma Aldrich was used as pore forming agent, to induce the formation of an additional macro and ultra-macro porosity with pore size > 50 nm and > 100 µm respectively, according to the IUPAC classification, following the reaction: $2H_2O_2$ (l) → $2H_2O$ (l) + O_2 (g).

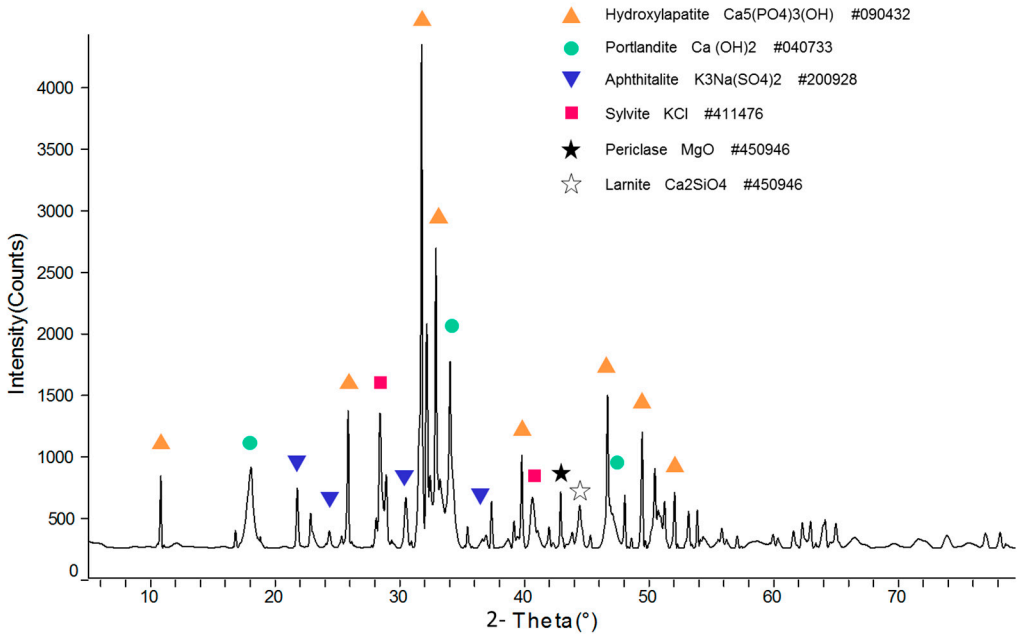

Figure 1. Phase composition of the biomass ash blend after thermal treatment at 900 °C.

Table 1. Elemental composition of BM after thermal treatment obtained from Energy Dispersive X-Ray Spectroscopy analysis.

Element	O	Ca	P	K	Cl	Si	Mg	Na	Fe	S	Al
[wt. %]	51.3	22.3	5.2	6.8	3.1	2.8	2.1	2.0	2.0	1.8	0.7

2.2. Sample Preparation

The metakaolin powder was added to the potassium silicate solution in a proper weight ratio to obtain a SiO_2: Al_2O_3 molar ratio equal to 4, then biomass ash blend was added in different amounts. As in a previous work [24], BM powder was added until constituting the 50 wt. % or 75 wt. % of the powder fraction, with the aim to maximize the volume of disposed waste material without affecting the final properties of the material and the geopolymerization process. The slurry was then mixed through mechanical stirring for 20 min and hydrogen peroxide solution was finally added to the mixture in measure of 5 wt. % on the total mass of the slurry, followed by further 1 min stirring (Table 2). A same volume of slurry for each sample was then poured in plastic square (60 mm × 60 mm, h = 25 mm) or cylindrical silicone (D = 51 mm, h = 65 mm) moulds, which were sealed and cured for 24 h in a heater at 60 °C, at relative humidity conditions of 45 ± 5%. The samples were then demoulded and dried at 60 °C for additional 12 h. The two investigated formulations were labelled as MKBM50 and MKBM75 according to the amount of biomass ash used (50% or 75% respectively, Table 2).

Table 2. Geopolymer mixture formulations.

Mixture	MK [wt. %]	BM [wt. %]	KS23 [wt. %]	H_2O_2 [wt. % on the Whole Mixture]
MKBM50	25.0	25.0	50.0	5
MKBM75	12.5	37.5	50.0	5

2.3. Characterization

In order to investigate the reaction degree of the geopolymers and the role played by biomass ashes in the samples microstructure, micrographs and EDS measurements were collected by Electron Microscopy FE-SEM (Carl Zeiss Sigma NTS, equipped with EDS probe X-Act, INCA Energy 300, Oxford Instruments, Abingdon, UK) and X-Ray diffraction patterns were obtained using a Powder Diffractometer Bruker D8 Advance with CuKα radiation (Karlsruhe, Germany).

The bulk density of the geopolymers was analytically determined by weight to volume ratio as the average on three cylindrical samples of diameter 51 mm, height 7 mm and true density values were obtained using a Helium pycnometer (Multivolume Pycnometer 1305, Micromeritics).

The open porosity in the range 0.0058–1000 μm was determined by Hg intrusion porosimetry (ThermoFinnigan 240), while total porosity was analytically calculated as the difference between true and bulk density according to the following formula: $P_t = (1 - \rho_b/\rho_t) \times 100\%$. The value for the remaining porosity, which includes open ultra-macro (>1000 μm) and closed porosity, was indirectly determined as the difference between total and open porosity.

Compressive strength of the geopolymer composites was determined as an average on 6 cylindrical samples with a diameter of 27 mm and a height of 38 mm using a cross-head speed of 2 mm/min by means of a Zwick Z050 testing machine (Zwick GmbH, Ulm, Germany).

The thermal stability and mass loss of the geopolymers was carried out by Simultaneous Thermal Analysis by means of a STA 449 Jupiter instrument (Netzsch Geraetebau, Selb, Germany) up to 1000 °C, with a heating rate of 10 °C/min and in dry air flux. Linear shrinkage at high temperature was determined with a Netzsch Dilatometer 402E (Netzsch, Selb, Germany) in air flux up to 1000 °C with a heating rate of 10 °C/min. Finally, thermal conductivity was measured at 30 °C on disks of 51 mm diameter and 7 mm thickness using the guarded heat flow meter DTC 300 (TA Instruments, New Castle, DE, USA) on pre-dried samples in a ventilated oven at 50 °C for 4 days.

3. Results and Discussion

3.1. Mineralogical Characterization

The diffraction patterns for cured MKBM50 and MKBM75 are plotted in Figure 2. The two samples are qualitatively similar in terms of phase composition of the reaction products, as for both formulations the detected crystalline phases mostly derive from the biomass ash, besides some traces of quartz, anatase and muscovite resulting from the metakaolin. The formation of the geopolymer phase is highlighted by the presence of the hump in the range of 20–36 degree of 2 θ in both samples, due to the alkali activation of the metakaolin fraction and formation of amorphous phases.

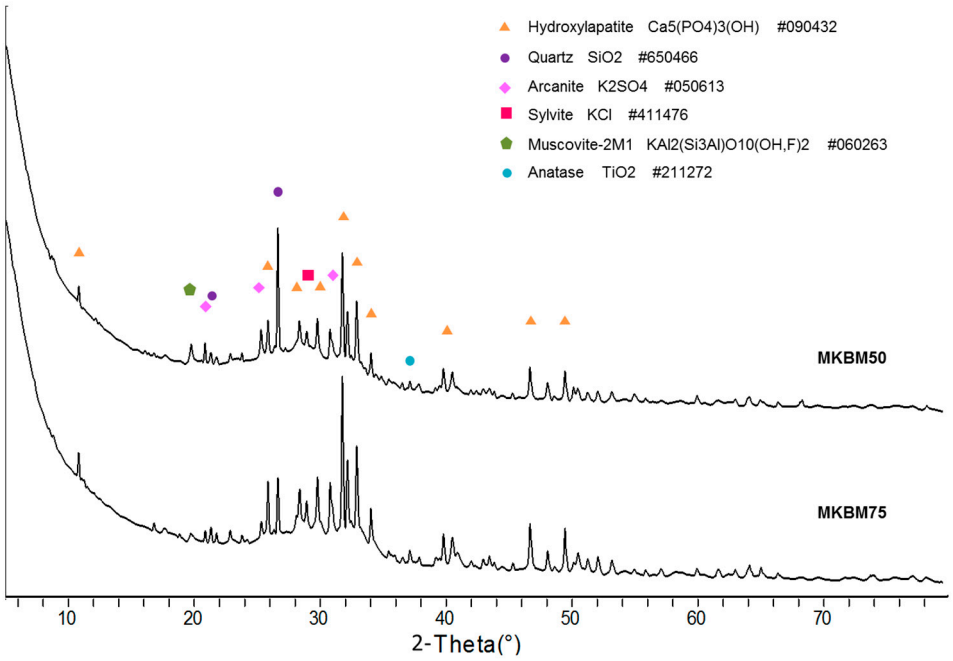

Figure 2. Phase composition of MKBM50 (top line) and MKBM75 (bottom line).

As can be noticed, the biomass ash did not actively participate in the formation of the reaction products of the geopolymer and its crystalline phases remained unchanged in the consolidated matrix, acting as a partially reactive filler. The effects of the alkaline activator only resulted in minor surface modifications on the biomass ash particles. Similar to BM raw powder, the main phases in both samples are represented by calcium phosphates, potassium chlorides and potassium sulphates. The only remarkable difference in the patterns of raw ashes and geopolymers relates to the absence of portlandite in the reacted materials. The absence of crystalline $Ca(OH)_2$ in the composites suggests the occurrence of a preferential reaction between unstable and reactive Ca from portlandite and the alkali silicate solution, likely forming amorphous hydrated gel phases within the geopolymer matrix or acting as an ionic substitution in the network of the alkali activated material [26,27].

Only minor differences were found between the spectra of the two composites, as both materials exhibited the same phase composition in qualitative terms. The only differences found related to the intensities of the peaks attributable to the presence of metakaolin (mainly quartz and muscovite) and the biomass (mainly hydroxyapatite, arcanite and sylvite), which appeared to be higher in sample MKBM50 and MKBM75, respectively.

3.2. Macro and Microstructural Characterization

The two obtained composites MKBM50 and MKBM75 are reported in Figure 3. The two materials appeared significantly different in their consistency and in the aspect of the developed porosity

network. The formulation with a lower amount of biomass ash, namely MKBM50, shows a cohesive macrostructure, with a uniformly distributed pore network without any sedimentation nor graduation effects. Some ultra-macro cavities up to 3.5 mm were detected due to the coalescence of smaller voids (Figure 3, left panel). Differently, the sample with a higher BM/MK ratio did not form a properly consolidated material and resulted in a layered macrostructure, with pores coalescence in the top, with cavities even of the order of centimetres and an incoherent crumbled bottom (Figure 3, right panel). This inhomogeneous appearance was due to the excessively low ratio of reactive to inert precursors in the mixture, which did not allow for the complete geopolymerization of the material. Furthermore, the low viscosity of the slurry derived from the presence of extra water, may have excessively lengthened the setting time and hindered the formation of a properly consolidated material. This caused a partial sedimentation of the BM and the collapse of the gas bubbles before the hardening of the slurry. The higher bulk density of MKBM75 compared to MKBM50 (545 kg/m^3 and 313 kg/m^3 respectively) directly results from the minor and non-uniform bloating of the sample, as can be seen from Figure 3.

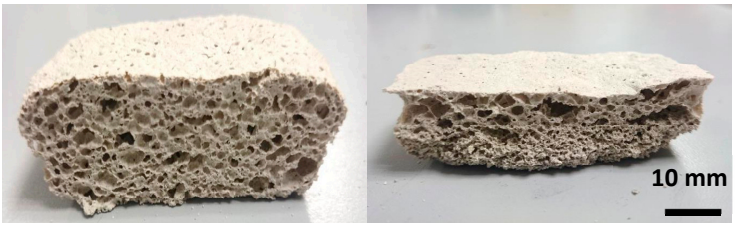

Figure 3. Cross section of MKBM50 (left) and MKBM75 (right) samples.

Despite the phase composition being comparable in the two samples, from a microstructural point of view the geopolymerization process led to the formation of two differently consolidated materials depending on the biomass ash amount, as evident from the micrographs reported in Figure 4. The MKBM50 formulation produced a homogeneously reacted material, whose microstructure is defined by the typical aluminosilicate nanoprecipitates derived from the alkali activation of the metakaolin powder (Figure 4a,b). The overall porosity is characterized by a uniformly distributed ultra-macropore network with cavities up to 3 mm wide (Figure 3), generated by the addition of hydrogen peroxide, along with a secondary order micrometric macroporosity, also including the window pores formed on the surface of the macro-cavities by the gas pressure and the intrinsic mesoporosity typical of geopolymer materials (Figure 4a,b).

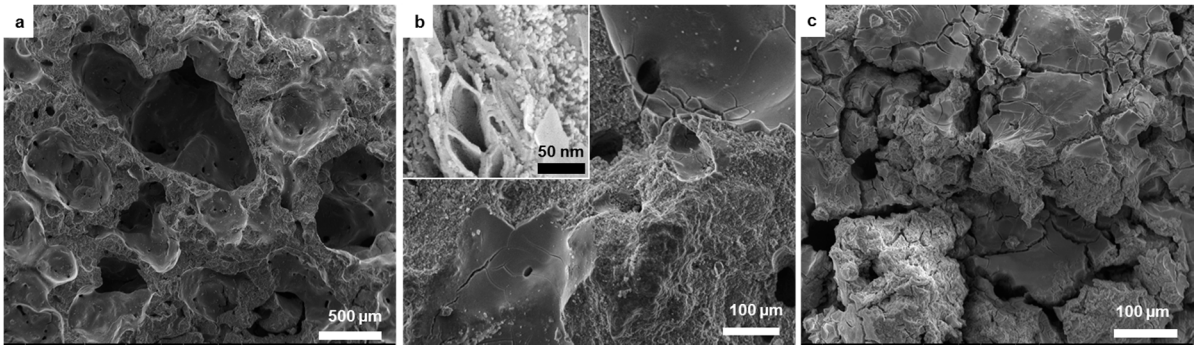

Figure 4. Microstructure of MKBM50 (**a**, **b**) and MKBM75 (**c**).

As previously noticed, BM remained mostly unreacted but strongly retained and integrated in the geopolymer matrix, which resulted well consolidated. Differently, the MKBM75 sample (Figure 4c) appeared widely cracked and incohesive in its porous upper section, due to the presence of an excess

of unreacted silicate, which was largely confined to the top of the material. The incohesive bottom layer of the sample was not examined, due to its scarce consistency.

From microstructural examinations, it was evidenced that neither of the two samples contained well defined hydrated phases as C–S–(A)–H integrated within the amorphous alkali aluminosilicate matrix, confirming what previously found from XRD analysis. This again suggests that Ca ions more likely embedded in the aluminosilicate network forming amorphous to semi-crystalline calcium-aluminosilicate reaction products [28], especially in the transition zone at the interface of the biomass ash unreacted grains. As previously found by other studies [27,29,30], in a system with moderate alkali conditions (SiO_2: K_2O = 2.0), the preferential reaction product is represented by an alkali-aluminosilicate-hydrated network (K–A–S–H), which in presence of Ca ions may exhibit ion exchange ability up to the complete incorporation of available Ca^{2+} as substitutes for K^+. As for MKBM50, the available Ca was probably not enough to act as extra nucleation sites for the growth of calcium-silicate hydrates, nor the calcium silicate phases as Ca_2SiO_4 were sufficient to generate a significant amount of C–S–H gel. The semi-quantitative elemental composition of the matrix obtained from EDS analysis on different sampling spots (Table 3) confirms the homogeneous distribution of dissolved Ca in the geopolymer network. As evident, Ca/Si, Si/Al and K/Al ratios lay in the ranges identified by Garcia-Lodeiro et al. for (Ca, K)–A–S–H structures [29].

Table 3. Elemental ratio composition of the geopolymer composites by EDS analysis (averaged on 4 analysis points). Data are reported net of an error of 10%.

Average Elemental Ratios [At. %]	MKBM50	MKBM75	(Ca, K)ASH Garcia-Lodeiro et al. [28]
Ca/Si	0.1	0.2	0 < Ca/Si < 0.3
Si/Al	2.1	2.8	1.2 < Si/Al < 10
K/Al	0.5	3.5	0 < K/Al < 1.9

Also for MKBM75 the obtained ratios indicate that no C–S–(A)–H phases have formed and the development of a Ca-substituted geopolymer network was rather favoured (Table 3). However, higher Si/Al and K/Al ratios confirm the presence of an excess of unreacted potassium silicate, which in turn confirms the scarce reactivity of the ashes in the alkali environment of the formulation. A more considerable amount of BM, which is far less reactive than MK towards alkali activation and, on the other hand, does not contain sufficient amounts of hydraulic phases that might bind the aqueous phase to form a proper C–S–H gel, resulted in the presence of extra water in MKBM75, which hindered the formation of a well reacted alkali-silicoaluminate network. Such extra water is quickly removed from the hardened material during the curing step, causing the formation of a higher volume of pores in the matrix and inducing diffuse cracking [27]. The formation of an underdeveloped three-dimensional polysialate network and the propagation of extensive cracks among the geopolymer matrix caused the fragmentation of the porous material, resulting in some cases in the complete spalling of debris and severe loss of cohesion [31].

Given the scarce consistency of MKBM75, the evaluation of the thermal properties and the suitability of the geopolymer composite to act as an insulating core was carried out only on MKBM50 formulation. As evident, a 50 wt. % of biomass ash in the powder fraction represents a sufficient amount which allows the volume of disposed ashes to be maximized, without compromising the properties of the final material.

3.3. Density, Pore Size Distribution and Compressive Strength

The obtained values of bulk (ρ_b) and true (ρ_t) density, open (P_o), total (P_t) and closed/unmeasured ($P_{c\text{-}u}$) porosity for MKBM50 sample are reported in Table 4. The pore size distribution is plotted in Figure 5 in terms of both total and relative pore volume. The calculated values of total porosity P_t and the corresponding bulk density are in accordance with data trends reported by other authors for

metakaolin and fly ash geopolymers foamed with different amounts of H_2O_2, comprised between 1.2 and 5.0 wt. % [18,32,33] or different amounts of Si or Al [15–21]: among the considered geopolymers, the biomass-based composite MKBM50 stands as one with the highest total porosity/bulk density ratio (Figure 6).

Table 4. Density, porosity and average pore diameter for MKBM50.

Sample	ρ_b [kg/m^3]	ρ_t [kg/m^3]	P_o [vol. %]	P_{c-u} [vol. %]	P_t [vol. %]	Median Pore Diameter (0.01–1000 μm) [μm]
MKBM50	313 ± 3	2288 ± 1	54.4	32.1	86.5	0.07

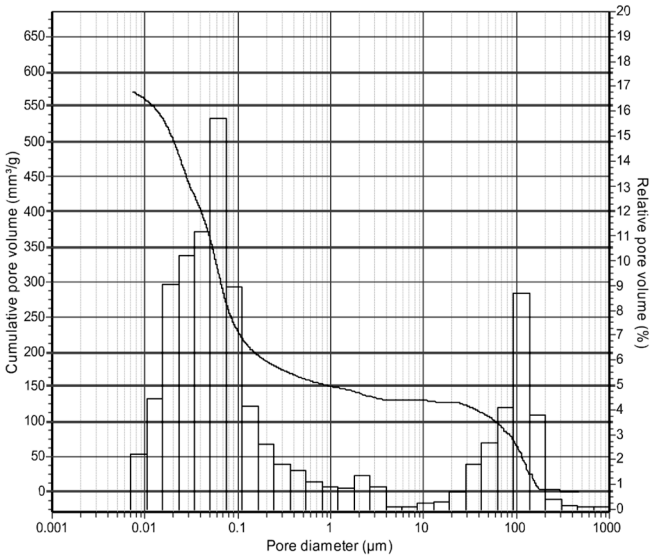

Figure 5. Open pore size distribution for MKBM50.

The reported histograms highlight a bimodal pore size distribution: more than 60% of the total pore volume lays in the diameter range between 0.007 μm and 0.1 μm and about 23% is determined by voids with equivalent diameter comprised between 20 μm and 200 μm. The former, narrower pore distribution defines the intrinsic mesoporosity of the geopolymer and does not depend on the addition of the pore forming agent. The latter is mainly defined by cell window pores and secondary interconnecting pores formed in the macro-cavities by gas release at high pressure and by ultra-macro voids (Figure 4a,b). Data are consistent with image analysis evaluations, from which macro and ultra-macropore dimensions appear in the range from about 150 μm to 3500 μm, with cell windows ranging from 20 μm to 80 μm. The reported data are in good agreement with the previous findings obtained by microstructural evaluations (Figure 4a,b) except for the contribution of the induced porosity by effects of H_2O_2, whose rate have been underestimated by the MIP analysis.

It should be noted that the instrumental limitations in the ultra-macro range and the non-optimal suitability of the sample, too little to include a representative fraction of ultra-macropores, might have resulted in an underestimated value of the open ultra-macro porosity. The fairly high value calculated for P_{c-u} clearly compensates for this underestimation. In fact, observing the irregular morphology of the formed voids and the bulk struts of the material (Figure 4a), it is reasonable to think that a significant fraction of the unmeasured porosity P_{c-u} is constituted by interconnected "ink-bottle" pore network, whose wider cavities are filled with mercury only at the intrusion pressure of the finer input apertures, leading to an evident underestimation of the wide pore volume and a consistent overestimation of the fine pore volume [34]. The 60 °C curing temperature could have accelerated the decomposition of the hydrogen peroxide and the setting speed of the slurry, therefore reducing

the uniformity of the formed cells and homogeneity of their distribution, promoting the formation of the "ink-bottle" porosity [18]. Furthermore, a less significant fraction of the unmeasured porosity is represented by nanopores smaller than 0.006 µm, as off the detection limit of the instrument.

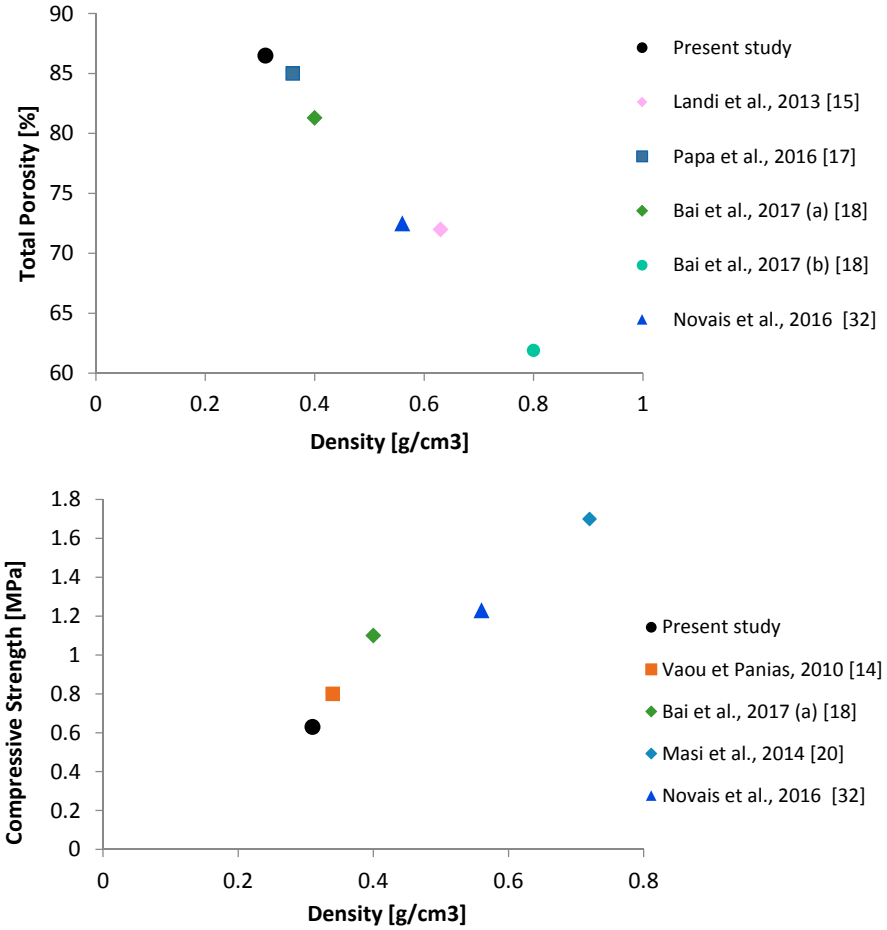

Figure 6. Total porosity/Density (upper panel) and Compressive strength/Density (lower panel) relationship for geopolymers from different literature studies.

The pore network of the geopolymer foam (volume, size and connectivity) strictly correlates with the density of the material and both these parameters, in turn depending on the specific amount of foaming agent used and the viscosity of the system, play a noticeable role in defining its mechanical properties. The calculated compressive strength for MKBM50 was of 0.63 ± 0.19 MPa, a value well-matched with the trend obtained from the literature on strength and density values of porous geopolymers (Figure 6). As can be noticed, MKBM50 stands out as a highly porous, low-density geopolymer, whose mechanical properties, albeit relatively low, are still acceptable to ensure the material adequate self-bearing and easy handling ability, in turn allowing for the coupling with protective fibre reinforced skins to form a sandwich insulating panel [25].

3.4. Thermal Properties

The thermal behaviour of MKBM50 up to 1000 °C in terms of mass loss, endo/exothermic reactions and linear shrinkage is reported in Figure 7. The composite underwent a significant mass loss of near 5.5 wt. % in the temperature range of 20–200 °C (upper panel), accompanied by a slight linear shrinkage of 0.1% (lower panel). These events are both related to the evaporation of the residual water and the desorption of water trapped in the pores. In the temperature range between 200 °C and 700 °C dehydroxylation occurs and water is removed from Si–OH and Al–OH groups, resulting

in a slight shrinkage and a mass loss of about 3.0% [35]. In this stage, the gradual decomposition of hydrated (Ca, K)–A–S–H type gels also occurs, being the mass loss event also related to the removal of chemical bound water from such gel structures [36,37].

In the final stage, from 800 °C to 1000 °C, the material started to densify via viscous flow, undergoing a significant linear shrinkage which exceeded 20% at 975 °C and accounting for more than 80% of the overall shrinkage of the material. In this temperature range the material experienced a further mass loss event, leading to a final mass loss of about 9.3 wt. %. Such findings are in good agreement with previous literature on thermal behaviour of K-based geopolymers [35]. As previously evidenced by XRD results, calcium mainly remained in the form of unreactive and thermally stable hydroxyapatite and only a minor part was integrated in the amorphous geopolymer gel structure, making the composite thermal properties similar to those previously reported for metakaolin-based geopolymers except for the extent of mass loss from dehydration/dehydroxylation of hydrated species [35,37].

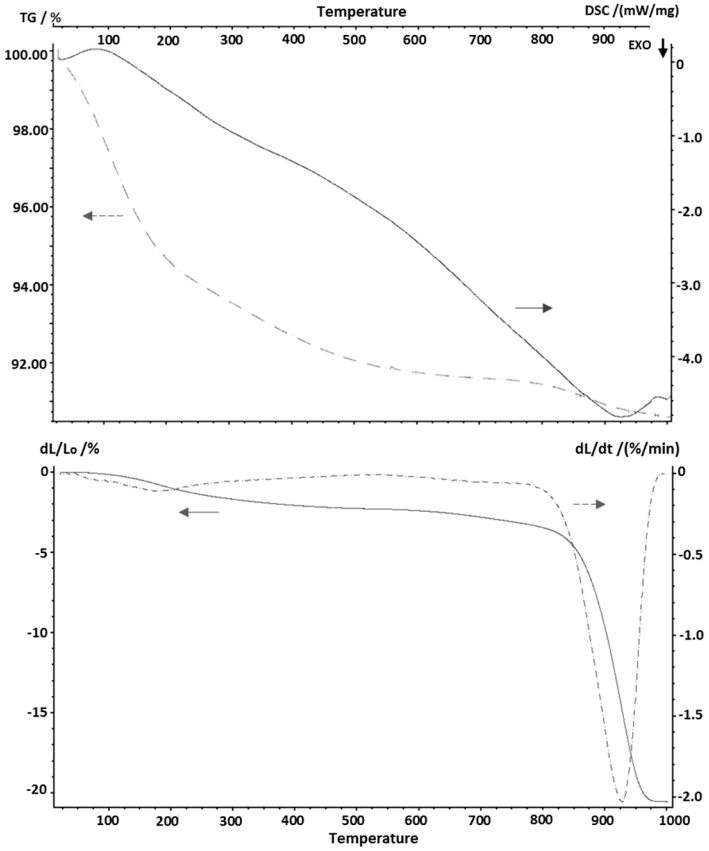

Figure 7. TG/DSC curves (top) and dilatometric curve with its derivative (bottom) for MKBM50.

The thermal conductivity of the material, calculated as the average on three samples, was of 0.073 W/mK at 30 °C for an average bulk density of 313 kg/m^3, a value in line with previous studies on alkali activated foams [18,32,33,38] and lower than other lightweight inorganic materials for thermal insulation such as aerated concrete [39,40]. As evidenced from many literature studies, the thermal conductivity of a porous material mainly relates with its density, a parameter which in turn is determined by different factors such as the solid/liquid ratio, the curing temperature, the addition of surfactants/foaming agents and the raw materials used [9,17,21,32,33]. The latter, however, seem to play a less significant role, as the results here obtained can be directly compared with those obtained different geopolymers, regardless the nature of the precursors. For example, Novais et al. obtained a porous geopolymer with a slightly higher density of 560 kg/cm^3, a higher compressive

strength of 1.23 MPa and a slightly higher thermal conductivity of 0.107 W/mK but using a lower amount of hydrogen peroxide in a biomass-based geopolymer [32]. Besides, Feng et al. used a similar amount of H_2O_2 in a fly ash-based geopolymer, obtaining comparable results in terms of density and thermal conductivity (335 kg/cm^3 and 0.082 W/mK, respectively) and a slightly higher compressive strength of 0.96 MPa [33]. As previously discussed, in the material investigated here the addition of 5 wt. % of H_2O_2 was sufficient to generate a macro-porosity made up of both cellular voids and wide irregular cavities, which contributed to different extent to lower the thermal conductivity of the material. By generating O_2 on decomposition, such H_2O_2 amount lead to an increase in the number of formed voids in the material, increasing its apparent porosity and correspondingly reducing its density and thermal conductivity values. The presence of a well-developed intrinsic porosity in the geopolymer struts and the presence of a wide number of cell windows in the cavities of the composite resulted in an extended network of interconnected voids in the range of meso/ macropores, which contributed to lower the density and thermal conductivity of the material without excessively affecting its mechanical properties. The designed biomass-based geopolymer therefore can outperform different materials commonly used in thermal insulating boards as for its thermal conductivity, bulk density and compressive strength values. In this regard, foamed concrete may exhibit a thermal conductivity equal or higher than 0.08 W/mK for a specific strength of about 1 KNm/kg, while MKBM50 showed a thermal conductivity of 0.073 W/mK for a specific strength around 2 KNm/kg [32].

4. Conclusions

The obtained results showed that a low-cost, value-added geopolymer can be easily produced using animal and vegetal derived biomass ash as a partially reactive precursor. The porous geopolymer composite produced with a blend of 50 wt. % waste ash and 50 wt. % metakaolin exhibited a well reacted microstructure, with the calcium-phosphate ashes homogeneously integrated in the aluminosilicate geopolymer matrix as partially reactive fillers. Such composition represented the best balance in terms of low density (313 kg/m^3) and mechanical strength (0.63 MPa), besides showing interesting thermal insulating ability, with a thermal conductivity of 0.07 W/mK at 30 °C and an outstanding thermal stability up to 800 °C. The biomass-metakaolin porous composite investigated here therefore appears as a promising thermal insulating material, suitable to be used as a lightweight heat barrier in such applications where mechanical performances are not a primary requirement, such as a core for thermostructural sandwich panels coupled with fibre reinforced laminated skins.

Acknowledgments: These activities and the project EEE-CFCC (2016–2018) are co-funded by the POR-FESR 2014–2020, Asse 1, Azione 1.2.2 of Emilia Romagna Region. Mattia Leonardi and G. De Aloysio from CertiMaC are kindly acknowledged for carrying out the thermal conductivity measurements. Tampieri Energie is acknowledged for providing the biomass ash.

Author Contributions: Claudio Mingazzini conceived the insulating sandwich panel and provided the fibre reinforced skins. Annalisa Natali Murri, Valentina Medri, Elettra Papa and Elena Landi conceived, designed and carried out the experiments for the insulating core; Luca Laghi set up and performed the thermal conductivity measurements; Annalisa Natali Murri analyzed the data and wrote the paper. Valentina Medri and Elena Landi revised the work.

Conflicts of Interest: The authors declare no conflict of interest.

References

1. Asdrubali, F.; D'Alessandro, F.; Schiavoni, S. A review of unconventional sustainable building insulation materials. *Sustain. Mater. Technol.* **2015**, *4*, 1–17. [CrossRef]
2. Schiavoni, S.; D'Alessandro, F.; Bianchi, F.; Asdrubali, F. Insulation materials for the building sector: A review and comparative analysis. *Renew. Sustain. Energy Rev.* **2016**, *62*, 988–1011. [CrossRef]
3. Sudareva, N.G.; Smyslova, L.A. Domestic heat-insulation materials for shipbuilding. *Russ. J. Gen. Chem.* **2010**, *80*, 2134–2142. [CrossRef]

4. Medri, V.; Papa, E.; Mazzocchi, M.; Laghi, L.; Morganti, M.; Francisconi, J.; Landi, E. Production and characterization of lightweight vermiculite/geopolymer-based panels. *Mater. Des.* **2015**, *85*, 266–274. [CrossRef]
5. Peacock, R.D.; Reneke, P.A.; Jones, W.W.; Bukowski, R.W.; Babrauskas, V. Concepts for fire protection of passenger rail transportation vehicles: Past, present and future. *Fire Mater.* **1995**, *19*, 71–87. [CrossRef]
6. Baetens, R.; Jelle, B.P.; Thue, J.V.; Tenpierik, M.J.; Grynning, S.; Uvsløkk, S.; Gustavsen, A. Vacuum insulation panels for building applications: A review and beyond. *Energy Build.* **2010**, *42*, 147–172. [CrossRef]
7. Fongang, R.T.T.; Pemndje, J.; Lemougna, P.N.; Chinje Melo, U.; Nanseu, C.P.; Nait-Ali, B.; Kamseu, E.; Leonelli, C. Cleaner production of the lightweight insulating composites: Microstructure, pore network and thermal conductivity. *Energy Build.* **2015**, *107*, 113–122. [CrossRef]
8. Natali Murri, A.; Medri, V.; Landi, E. Production and thermomechanical characterization of wool–geopolymer composites. *J. Am. Ceram. Soc.* **2017**, *100*, 2822–2831. [CrossRef]
9. Kamseu, E.; NGouloure, Z.N.M.; Nait-Ali, B.; Zekeng, S.; Melo, U.C.; Rossignol, S.; Leonelli, C. Cumulative pore volume, pore size distribution and phases percolation in porous inorganic polymer composites: Relation microstructure and effective thermal conductivity. *Energy Build.* **2015**, *88*, 45–56. [CrossRef]
10. Lyon, R.E.; Balaguru, P.N.; Foden, A.; Sorathia, U.; Davidovits, J.; Davidovics, M. Fire-resistant aluminosilicate composites. *Fire Mater.* **1997**, *21*, 67–73. [CrossRef]
11. Davidovits, J. *Geopolymer Chemistry and Applications*, 2nd ed.; Geopolymer Institute: Saint Quentin, France, 2008; ISBN 9782951482098.
12. Duxson, P.; Fernández-Jiménez, A.; Provis, J.L.; Lukey, G.C.; Palomo, A.; van Deventer, J.S.J. Geopolymer technology: The current state of the art. *J. Mater. Sci.* **2007**, *42*, 2917–2933. [CrossRef]
13. Kriven, W.M.; Bell, J.L.; Gordon, M. Microstructure and microchemistry of fully-reacted geopolymers and geopolymer matrix composites. *Ceram. Trans.* **2003**, *153*, 227–250. [CrossRef]
14. Vaou, V.; Panias, D. Thermal insulating foamy geopolymers from perlite. *Miner. Eng.* **2010**, *23*, 1146–1151. [CrossRef]
15. Landi, E.; Medri, V.; Papa, E.; Dedecek, J.; Klein, P.; Benito, P.; Vaccari, A. Alkali-bonded ceramics with hierarchical tailored porosity. *Appl. Clay Sci.* **2013**, *73*, 56–64. [CrossRef]
16. Medri, V.; Papa, E.; Dedecek, J.; Jirglova, H.; Benito, P.; Vaccari, A.; Landi, E. Effect of metallic Si addition on polymerization degree of foamed alkali-aluminosilicates. *Ceram. Int.* **2013**, *39*, 7657–7668. [CrossRef]
17. Papa, E.; Medri, V.; Kpogbemabou, D.; Morinière, V.; Laumonier, J.; Vaccari, A.; Rossignol, S. Porosity and insulating properties of silica-fume based foams. *Energy Build.* **2016**, *131*, 223–232. [CrossRef]
18. Bai, C.; Colombo, P. High-porosity geopolymer membrane supports by peroxide route with the addition of egg white as surfactant. *Ceram. Int.* **2017**, *43*, 2267–2273. [CrossRef]
19. Hajimohammadi, A.; Ngo, T.; Mendis, P.; Sanjayan, J. Regulating the chemical foaming reaction to control the porosity of geopolymer foams. *Mater. Des.* **2017**, *120*, 255–265. [CrossRef]
20. Masi, G.; Rickard, W.D.A.; Vickers, L.; Bignozzi, M.C.; van Riessen, A. A comparison between different foaming methods for the synthesis of light weight geopolymers. *Ceram. Int.* **2014**, *40*, 13891–13902. [CrossRef]
21. Kamseu, E.; Nait-Ali, B.; Bignozzi, M.C.; Leonelli, C.; Rossignol, S.; Smith, D.S. Bulk composition and microstructure dependence of effective thermal conductivity of porous inorganic polymer cements. *J. Eur. Ceram. Soc.* **2012**, *32*, 1593–1603. [CrossRef]
22. Komnitsas, K.A. Potential of geopolymer technology towards green buildings and sustainable cities. *Procedia Eng.* **2011**, *21*, 1023–1032. [CrossRef]
23. Natali Murri, A.; Medri, V.; Ruffini, A.; Papa, E.; Landi, E. Study of the chemical activation of hydroxyapatite rich ashes as raw materials for geopolymers. *Ceram. Int.* **2015**, *41*, 9734–9744. [CrossRef]
24. Natali Murri, A.; Medri, V.; Piancastelli, A.; Vaccari, A.; Landi, E. Production and characterization of geopolymer blocks based on hydroxyapatite rich biomass ashes. *Ceram. Int.* **2015**, *41*, 12811–12822. [CrossRef]
25. Mingazzini, C.; Scafè, M.; Mazzanti, F.; Bezzi, F.; Giorgini, L.; Zattini, G.; D'Angelo, E.; Laghi, L.; De Aloysio, G.; Bandini, S. Flame resistant composite panels processed from Preceramic Prepregs. In Proceedings of the 15th Conference & Exhibition of the European Ceramic Society ECERS 2017, Budapest, Hungary, 9–13 July 2017.
26. Granizo, M.L.; Alonso, S.; Blanco-Varela, M.T.; Palomo, A. Alkaline Activation of Metakaolin: Effect of Calcium Hydroxide in the Products of Reaction. *J. Am. Ceram. Soc.* **2002**, *85*, 225–231. [CrossRef]

27. Yip, C.K.; Lukey, G.C.; van Deventer, J.S.J. The coexistence of geopolymeric gel and calcium silicate hydrate at the early stage of alkaline activation. *Cem. Concr. Res.* **2005**, *35*, 1688–1697. [CrossRef]
28. MacKenzie, K.J.D.; Smith, M.E.; Wong, A. A multinuclear MAS NMR study of calcium-containing aluminosilicate inorganic polymers. *J. Mater. Chem.* **2007**, *17*, 5090–5096. [CrossRef]
29. Garcia-Lodeiro, I.; Palomo, A.; Fernández-Jiménez, A.; Macphee, D.E. Compatibility studies between N-A-S-H and C-A-S-H gels. Study in the ternary diagram NaO–CaO–AlO–SiO–HO. *Cem. Concr. Res.* **2011**, *41*, 923–931. [CrossRef]
30. Puligilla, S.; Mondal, P. Role of slag in microstructural development and hardening of fly ash-slag geopolymer. *Cem. Concr. Res.* **2013**, *43*, 70–80. [CrossRef]
31. Khan, M.Z.N.; Shaikh, F.A.; Hao, Y.; Hao, H. Synthesis of high strength ambient cured geopolymer composite by using low calcium fly ash. *Constr. Build. Mater.* **2016**, *125*, 809–820. [CrossRef]
32. Novais, R.M.; Buruberri, L.H.; Ascensão, G.; Seabra, M.P.; Labrincha, J.A. Porous biomass fly ash-based geopolymers with tailored thermal conductivity. *J. Clean. Prod.* **2016**, *119*, 99–107. [CrossRef]
33. Feng, J.; Zhang, R.; Gong, L.; Li, Y.; Cao, W.; Cheng, X. Development of porous fly ash-based geopolymer with low thermal conductivity. *Mater. Des.* **2015**, *65*, 529–533. [CrossRef]
34. Roels, S.; Elsen, J.; Carmeliet, J.; Hens, H. Characterization of pore structure by combining mercury porosimetry and micrography. *Mater. Struct.* **2001**, *34*, 76–82. [CrossRef]
35. Bell, J.L.; Driemeyer, P.E.; Kriven, W.M. Formation of ceramics from metakaolin-based geopolymers. Part II: K-based geopolymer. *J. Am. Ceram. Soc.* **2009**, *92*, 607–615. [CrossRef]
36. Gao, X.; Yu, Q.L.; Brouwers, H.J.H. Reaction kinetics, gel character and strength of ambient temperature cured alkali activated slag-fly ash blends. *Constr. Build. Mater.* **2015**, *80*, 105–115. [CrossRef]
37. Natali Murri, A.; Rickard, W.D.A.; Bignozzi, M.C.; van Riessen, A. High temperature behavior of ambient cured alkali-activated materials based on ladle slag. *Cem. Concr. Res.* **2013**, *43*, 51–61. [CrossRef]
38. Henon, J.; Alzina, A.; Absi, J.; Smith, D.S.; Rossignol, S. Potassium geopolymer foams made with silica fume pore forming agent for thermal insulation. *J. Porous Mater.* **2013**, *20*, 37–46. [CrossRef]
39. Narayanan, N.; Ramamurthy, K. Structure and properties of aerated concrete: A review. *Cem. Concr. Compos.* **2000**, *22*, 321–329. [CrossRef]
40. Hamad, A.J. Materials, production, properties and application of aerated lightweight concrete: Review. *Int. J. Mater. Sci. Eng.* **2014**, *2*, 152–157. [CrossRef]